

# Use of Rapid Reduced Electric Field Switching to Enhance Compound Specificity for Proton Transfer Reaction-Mass Spectrometry

González-Méndez, R, Watts, P, Reich, DF, Mullock, SJ, Cairns, S, Hickey, P, Brookes, M & Mayhew, CA

Author post-print (accepted) deposited by Coventry University's Repository

**Original citation & hyperlink:**

González-Méndez, R, Watts, P, Reich, DF, Mullock, SJ, Cairns, S, Hickey, P, Brookes, M & Mayhew, CA 2018, 'Use of Rapid Reduced Electric Field Switching to Enhance Compound Specificity for Proton Transfer Reaction-Mass Spectrometry' *Analytical Chemistry*, vol 90, no. 9, pp. 5664-5770.

<https://dx.doi.org/10.1021/acs.analchem.7b05211>

DOI [10.1021/acs.analchem.7b05211](https://dx.doi.org/10.1021/acs.analchem.7b05211)

ISSN 0003-2700

ESSN 1520-6882

Publisher: [American Chemical Society](#)

**Copyright © and Moral Rights are retained by the author(s) and/ or other copyright owners. A copy can be downloaded for personal non-commercial research or study, without prior permission or charge. This item cannot be reproduced or quoted extensively from without first obtaining permission in writing from the copyright holder(s). The content must not be changed in any way or sold commercially in any format or medium without the formal permission of the copyright holders.**

**This document is the author's post-print version, incorporating any revisions agreed during the peer-review process. Some differences between the published version and this version may remain and you are advised to consult the published version if you wish to cite from it.**

1 **Use of Rapid Reduced Electric Field Switching to Enhance Compound**  
2 **Specificity for Proton Transfer Reaction-Mass Spectrometry**

3

4 Ramón González-Méndez,<sup>1†</sup> Peter Watts,<sup>1</sup> D. Fraser Reich,<sup>2</sup> Stephen J. Mullock,<sup>2</sup> Stuart  
5 Cairns,<sup>3</sup> Peter Hickey,<sup>3</sup> Matthew Brookes,<sup>4</sup> and Chris A. Mayhew<sup>1,5\*</sup>

6

7 1. Molecular Physics Group, School of Physics and Astronomy, University of  
8 Birmingham, Edgbaston, Birmingham, B15 2TT, UK

9 2. Kore Technology Ltd, Cambridgeshire Business Park, Ely, Cambridgeshire, CB7  
10 4EA, UK

11 3. Defence Science and Technology Laboratory, Fort Halstead, Sevenoaks, Kent, TN14  
12 7BP, UK

13 4. Defence Science and Technology Laboratory, Porton Down, Salisbury, Wilshire SP4  
14 0JQ, UK

15 5. Institut für Atemgasanalytik, Leopold-Franzens-Universität Innsbruck, Rathausplatz  
16 4, 6850, Dornbirn, Austria

17

18 \* Corresponding author:

19 Tel.: +44 121 414 4729/ 0043 512 504 27783

20 E-mail: c.mayhew@bham.ac.uk/christopher.mayhew@uibk.ac.at

21

22 Key words: PTR-MS; explosives; reduced electric field; collisional induced dissociation

23

24

25

26

27

28

29

30

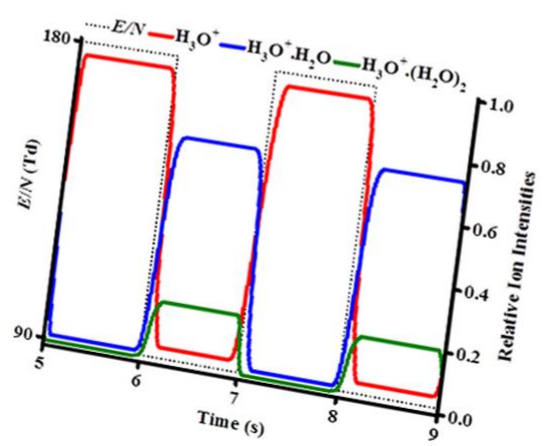
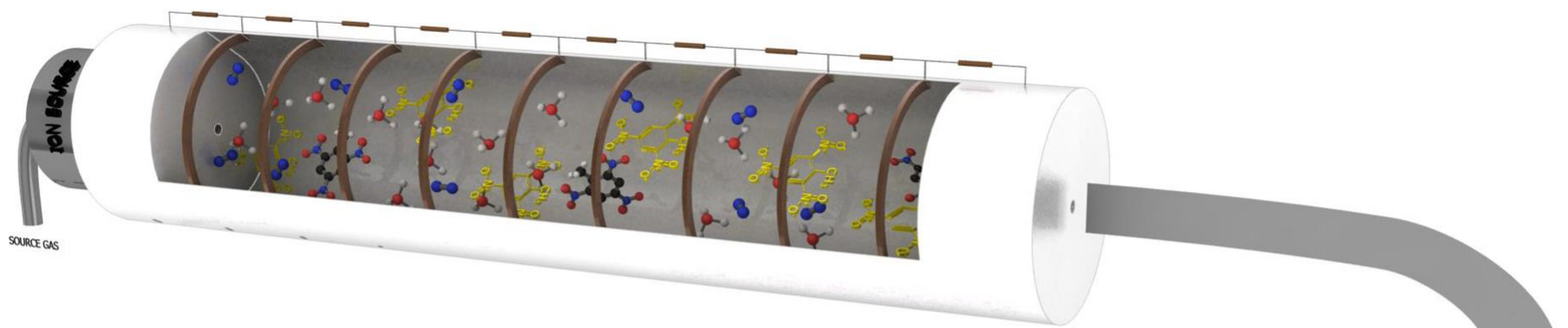
31

32 † Current address: Centre for Agroecology, Water and Resilience, Coventry University,  
33 Coventry, CV1 5FB, UK

34 Graphical abstract

35

36



37

38 **Abstract (250 words)**

39 The high sensitivity of Proton Transfer Reaction-Mass Spectrometry (PTR-MS) makes it a  
40 suitable analytical tool for detecting trace compounds. Its specificity is primarily determined  
41 by the accuracy of identifying the  $m/z$  of the product ions specific to a particular compound.  
42 However, specificity can be enhanced by changing the product ions (concentrations and types)  
43 through modifying the reduced electric field. For current PTR-MS systems this is not possible  
44 for trace compounds that would only be present in the reaction chamber of a PTR-MS for a  
45 short time (seconds). For such circumstances it is necessary to change the reduce electric field  
46 swiftly if specificity enhancements are to be achieved. In this paper we demonstrate such a  
47 novel approach, which permits any compound that may only be present in the drift tube for  
48 seconds to be thoroughly investigated. Specifically, we have developed hardware and software  
49 which permits the reaction region's voltages to be rapidly switched at a frequency of 0.1-5 Hz.  
50 We show how this technique can be used to provide a higher confidence in the identification  
51 of compounds than is possible by keeping to one reduced electric field value through  
52 illustrating the detection of explosives. Although demonstrated for homeland security  
53 applications, this new technique has applications in other analytical areas and disciplines where  
54 rapid changes in a compound's concentration can occur, e.g. in the Earth's atmosphere, plant  
55 emissions and in breath. Importantly, this adaptation provides a method for improved  
56 selectivity without expensive instrumental changes or the need for high mass resolution  
57 instruments.

58

59 Proton Transfer Reaction-Mass Spectrometry (PTR-MS) is a broad-based technique that has  
60 proved its analytical use in many fields including atmospheric chemistry, food science, breath  
61 analysis and Homeland Security.<sup>1</sup> Within the Homeland Security area, PTR-MS is capable of  
62 detecting a wide range of dangerous substances, and a number of studies have been published  
63 dealing with chemical warfare agents, illicit drugs and explosives.<sup>2-19</sup> A key criterion for any  
64 analytical instrumentation is sensitivity. The high sensitivity of PTR-MS, which can now reach  
65 levels of parts per quadrillion by volume in seconds,<sup>20</sup> permits the relatively easy detection of  
66 many chemical compounds in trace amounts.

67 While high sensitivity is necessary for a range of applications, high selectivity is also  
68 required so that chemical compounds can be identified with a high level of confidence in real-  
69 time. Higher selectivity is particularly needed with increasing sensitivity because the number  
70 of possible interferents at detectable levels increases. High chemical specificity is of  
71 considerable importance to the military, to emergency responders and for applications in  
72 security areas such as airports, harbours and train stations, where false alarms can cause  
73 significant cost and disruption to the public.

74 Without a pre-separation stage (e.g. a Gas Chromatography (GC) stage), PTR-MS  
75 primarily relies on the value of  $m/z$  of the product ion(s) to identify a given chemical compound.  
76 This results in an uncertainty in identification. Fast GC systems are being developed for use  
77 with PTR-MS to reduce any ambiguity in assignment, but these still take away from a major  
78 advantage of PTR-MS, namely real-time measurements.

79 A possible way to improve selectivity without losing the real-time capability advantage  
80 of PTR-MS is to manipulate the ion chemistry occurring in the reaction chamber. Thus different  
81 product ions (or changes in their intensities) can be used to aid in compound identification. A  
82 number of methods to achieve this have been proposed and adopted. One method is to use  
83 different reagent ions, e.g. changing from  $\text{H}_3\text{O}^+$  (proton transfer reactions) to  $\text{O}_2^+$  (charge  
84 transfer) to produce different product ions.<sup>13</sup> This is achieved by switching the reagent gas from  
85 water to air. Given that the reactions of  $\text{O}_2^+$  and  $\text{H}_3\text{O}^+$  with a neutral compound results in  
86 different product ions, rather than switching reagent ions,<sup>13-16</sup> it may be more beneficial for  
87 improved selectivity to have both (or more) reagent ions injected into the reaction chamber  
88 simultaneously, as recently illustrated by Amador-Muñoz et al.<sup>21</sup>

89 A more recent proposition to improve selectivity is the use of a RF ion funnel system  
90 to enhance collisional induced dissociation (CID).<sup>18,19</sup> Changes in CID can also be achieved by  
91 changing the reduced electric field, which is the key operational parameter in PTR-MS, and is  
92 the ratio of the electric field  $E$  in the drift tube to the total neutral number density  $N$ . By

93 changing the reduced electric field from a low value, for example 80 Td, to a high value, for  
94 example 180 Td (or vice-versa) differences in product ion distributions will occur. This can aid  
95 in the identification of the trace neutral responsible for those ions. This approach was used in  
96 the early investigations using PTR-MS,<sup>22,23</sup> where changes in the reduced electric field were  
97 used to distinguish isomeric compounds. More recent examples exploiting this technique can  
98 be found in the literature,<sup>24-26</sup> and this same approach was used by González-Méndez *et al.* to  
99 discriminate between nitro-glycerine (NG) and the isobaric compound 2,4,6-trinitrotoluene  
100 (TNT).<sup>17</sup> For that study the drift tube voltage was changed manually. However, for the  
101 switching of the reduced electric field to be analytically useful, the reduced electric field needs  
102 to be changed at a frequency whose reciprocal is comparable to the sample time of a compound  
103 in the drift tube. This is particularly the case for areas of application where the sample is present  
104 in the reaction chamber of a PTR-MS for short periods of time, e.g. a real-time breath sample  
105 (< 10 s) or for thermally desorbed materials such explosives (< 20 s).

106 The simplest way to provide a rapid change in  $E/N$  is to alter the  $E$  field by changing  
107 the voltage applied across the drift tube. In this paper we present details of a collaborative  
108 project involving Kore Technology Ltd. (Ely, UK), the Defence Science and Technology  
109 Laboratory and the University of Birmingham on new hardware and software modifications  
110 for such a purpose. We illustrate the application of this new development to a number of  
111 explosive, or explosive-related compounds, namely 2,4- and 2,6-dinitrotoluene (2,4- and 2,6-  
112 DNT,  $m/z$  182.03,  $C_7H_6N_2O_4$ ), hexamethylene triperoxide diamine (HMTD,  $m/z$  208.07,  
113  $C_6H_{12}N_2O_6$ ), and 1,3,5-trinitroperhydro-1,3,5-triazine (RDX,  $m/z$  222.04,  $C_3H_6N_6O_6$ ). These  
114 have been selected to show the application of the system for chemical compounds with  
115 different physical properties, such as vapour pressures, and chemical functional groups.

116 Finally, we comment that it may be even more beneficial for selectivity improvements  
117 to have the combined operation of a radio frequency ion-funnel PTR-MS and fast drift tube  
118 voltage switching. This is exemplified in this study for 2,4,6-trinitrotoluene (TNT,  $m/z$  227.02,  
119  $C_7H_5N_3O_6$ ).

120

## 121 **Methods**

122 **Experimental Details.** A Kore Technology Ltd. Proton Transfer Reaction-Time of Flight-  
123 Mass Spectrometry (PTR-ToF-MS) was used, details of which have been comprehensively  
124 described elsewhere.<sup>27, 28</sup> In brief, a needle valve is used to introduce water vapour from a  
125 container into a hollow cathode discharge source where, after ionisation via electron impact  
126 and subsequent ion-molecule processes, the terminal reagent ions are predominantly  $H_3O^+$  (or

127 at low  $E/N < 80$  Td protonated water clusters). These ions are transferred from the ion source  
128 into the reaction chamber, also referred to as the drift tube (DT), of the PTR-ToF-MS, where  
129 they encounter the analyte.  $\text{H}_3\text{O}^+$  efficiently reacts with an analyte M through proton transfer  
130 providing M has a proton affinity greater than that of water ( $\text{PA}(\text{H}_2\text{O}) = 691 \text{ kJ mol}^{-1}$ ).  
131 Proton transfer from the protonated water clusters will only occur if PA (M) is higher than  
132 that of the water clusters, which possess higher proton affinities than  $\text{H}_2\text{O}$ . For example, the  
133 proton affinity of the water dimer is  $808 \text{ kJ mol}^{-1}$ . If  $\text{PA}(\text{H}_2\text{O}) < \text{PA}(\text{M}) < \text{PA}(\text{H}_2\text{O})_2$ , as is the  
134 case for many explosives, then as the concentration of  $\text{H}_3\text{O}^+$  decreases at low  $E/N$  then the  
135 concentrations of the product ions must also decrease, but this is somewhat compensated by  
136 the increased reaction time. In this study, only HMTD has a proton affinity greater than that  
137 of water clusters.

138 Proton transfer can be non-dissociative (resulting in the protonated parent molecule  
139  $\text{MH}^+$ ) and/or dissociative. Dissociative proton transfer results in product ions which, depending  
140 on their  $m/z$  values, may be useful for the identification of a compound. Fragmentation may be  
141 spontaneous upon proton transfer or may require additional energy which is supplied through  
142 numerous collisions with the buffer gas during the migration of the product ions down the drift  
143 tube under the influence of the electric field,  $E$ .

144 The instrument's DT used in this study also incorporates a radio-frequency ion funnel  
145 (RFIF).<sup>18, 29</sup> In brief the RFIF consists of 29 stainless steel plates of 0.2 mm thickness, mounted  
146 on precision-machined ceramic rods at an even spacing of 3.2 mm per plate. Tabs on the  
147 electrodes permit a resistor chain on a ceramic strip to be connected in addition to two capacitor  
148 stacks which allow the RF to be applied to the second half of the reactor. The orifice diameters  
149 of the plates through the first half of the stack is 40 mm, as used in the standard drift tube  
150 reactor. In the second half of the DT the orifice diameter steadily decreases to 6 mm at the final  
151 plate before the exit aperture. Across the complete ion-funnel a DC voltage is applied driving  
152 ions axially. When just operating with only this voltage we shall refer to the instrument as  
153 operating in DC-only mode. To the second part of the drift tube a RF field can applied. The  
154 resonant frequency used is  $\sim 760 \text{ kHz}$  and the voltage amplitude (peak-to-peak) is 200 V. The  
155 RF field is superimposed on the DC voltage gradient across the complete drift tube. We shall  
156 refer to operating the instrument with the RF on as RF-mode, and its use in this paper is  
157 exemplified for TNT only.

158 At the end of the drift tube there is an exit plate which has at its centre a  $400 \mu\text{m}$   
159 aperture, through which a proportion of the reagent and product ions enter the ion transfer lens

160 section and then, after appropriate lensing, onwards to the pulser section, from which ions are  
161 pulsed into to the time-of-flight mass spectrometer for detection.

162 **Fast Reduced Electric Field Switching.** New electronics were developed by Kore  
163 Technology Ltd. for the purpose of providing fast reduced electric field switching that can be  
164 retrofitted into any Kore PTR-ToF-MS. The fast reduced electric field switching is  
165 accomplished by software control of a programmable +500 volt power supply unit (PSU). This  
166 can be controlled over the range 50 to 450 volts (covering typically the  $E/N$  range of between  
167 approximately 10 and 250 Td). It is possible to switch the output voltage according to the two  
168 required  $E/N$  values. This is achieved using a digital-to-analogue converter that allows a new  
169 software interface to set the two voltage values between which the power supply will switch.  
170 In addition to the voltage control, the software also provides the facility to alter the frequency  
171 of switching between two voltages. The data are saved as two separate, cumulative spectra  
172 from the two  $E/N$  states.

173 The circuitry for the switching has been added to an existing set of electronics that was  
174 not designed for switching. Oscilloscope traces of the power supply output (only) show  
175 asymmetry in the rise and fall times of the voltage. This is due to built-in diode circuitry on the  
176 output of the power supply. If we define the period between a stable low voltage and a stable  
177 high voltage after switching as the rise and fall times, we observe times of  $\sim 10$  ms and  $\sim 25$   
178 ms, respectively. When the power supply is connected to the reactor, thus adding resistors and  
179 capacitors to the output, by the same criterion we observe greater time differences in the rise  
180 and fall times of the product ions (see section 3.1 for details). Analytically what is important is  
181 that data are acquired when the product ion signal is constant in the two phases. This is  
182 accomplished by means of using purposely written software that censors the data between  
183 voltage changes.

184 **Operational parameters.** Explosives measurements were obtained through the use of  
185 PTFE swabs (ThermoFisher Scientific) doped with known quantities of explosives and placed  
186 into a Kore Technology Ltd. thermal desorption unit (TDU), which was connected to the inlet  
187 of the PTR-ToF-MS. Details of the TDU have been given elsewhere.<sup>17</sup> The swabs came  
188 prepared from the manufacturer mounted on rectangular cardboard for easy insertion into the  
189 TDU. Once a seal was created, a carrier gas (in this study laboratory air) was heated to the  
190 temperature of the TDU before it flows through a series of holes in a heated metal plate. This  
191 heated air then passed through the swab and into the inlet system driving any desorbed material  
192 through to the drift tube creating a concentration “pulse” of typically between 10 – 20 seconds  
193 of an explosive in the drift tube.<sup>17</sup>



194 Passivated (SilcoNert®) stainless steel inlet lines were used in order to minimise  
195 adsorption effects. All measurements were taken under the same operational conditions. The  
196 TDU, inlet tubing and drift tube were maintained at 150 °C. The drift tube pressure was set at  
197 1.1 mbar. The only variable was the operating drift tube voltage, which was changed to provide  
198 the appropriate reduced electric fields to yield the product ion(s) of interest for each explosive  
199 investigated.

200 For the fast switching experiments, the acquisition time per point was set to 40 ms. Such  
201 short acquisition times imply that ion counts fluctuations will be at the level of 15 to 20% due  
202 to ion count statistics. However, in real operation it is not necessary to present a signal that has  
203 not been processed. It is better to show for each individual cycle average ion signals outside of  
204 the circuit's time constants (i.e. after the rise and before the fall time), and that is what is  
205 presented in this paper, other than for one data set to illustrate the typical level of fluctuation  
206 observed in the signal intensities for 40 ms acquisition times over a cycle (see section 3.1).

207 **Explosive Compounds.** Explosive standards were purchased from AccuStandard Inc.,  
208 New Haven, CT. and diluted in the appropriate solvent(s) (HPLC grade) to provide the  
209 required quantity. Typically, the measurements were undertaken with between 1 and 50 ng of  
210 explosives deposited on the swabs prior to their insertion into the TDU to give an idea of  
211 realistic measurements.

212 **Density Functional Theory Calculations.** Density Functional Theory (DFT) calculations  
213 have been undertaken to determine the proton affinities and gas-phase basicities for the  
214 reactions of HMTD and RDX. These were obtained using the Gaussian09W program with the  
215 GaussView05 interface,<sup>30</sup> and the B3LYP functional with 6-31+G(d,p) basis set.

216

## 217 **Results and Discussion**

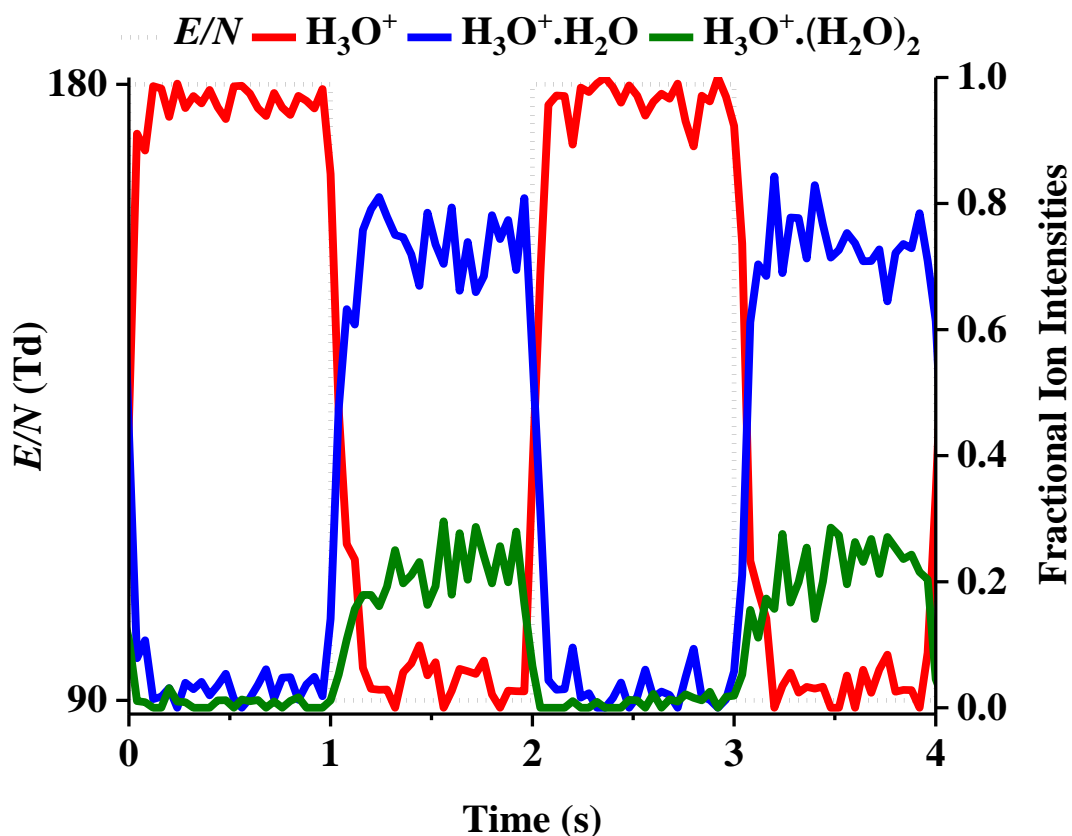
218 **Reagent Ions.** Before conducting any switching experiments with samples, it was important  
219 to characterise the time constants associated with the rapid change of voltages applied to the  
220 drift tube. To investigate this, we examined the temporal profile of the protonated water  $\text{H}_3\text{O}^+$   
221 ( $m/z$  19.02) and the dimer and trimer protonated water clusters,  $\text{H}_3\text{O}^+\cdot\text{H}_2\text{O}$  ( $m/z$  37.03) and  
222  $\text{H}_3\text{O}^+(\text{H}_2\text{O})_2$  ( $m/z$  55.04), respectively. These were chosen because their individual  
223 concentrations in the drift tube are very sensitive to the  $E/N$  value used. For example, at 90 Td  
224 protonated water clusters are the dominant reagent ions, whereas at 180 Td these have  
225 negligible intensities because the collisions occurring in the drift tube are sufficient to break-  
226 up protonated water clusters to the  $\text{H}_3\text{O}^+$  monomer. It should however be appreciated that the  
227 relative intensities of the reagent ions recorded are those measured at the detector. The actual

228 distribution of reagent ions in the drift tube may be different owing to possible break-up of the  
229 protonated water clusters in the transfer optics from the DT to the mass spectrometer and as a  
230 result of the dependence of the transmission of the ions on  $m/z$ .

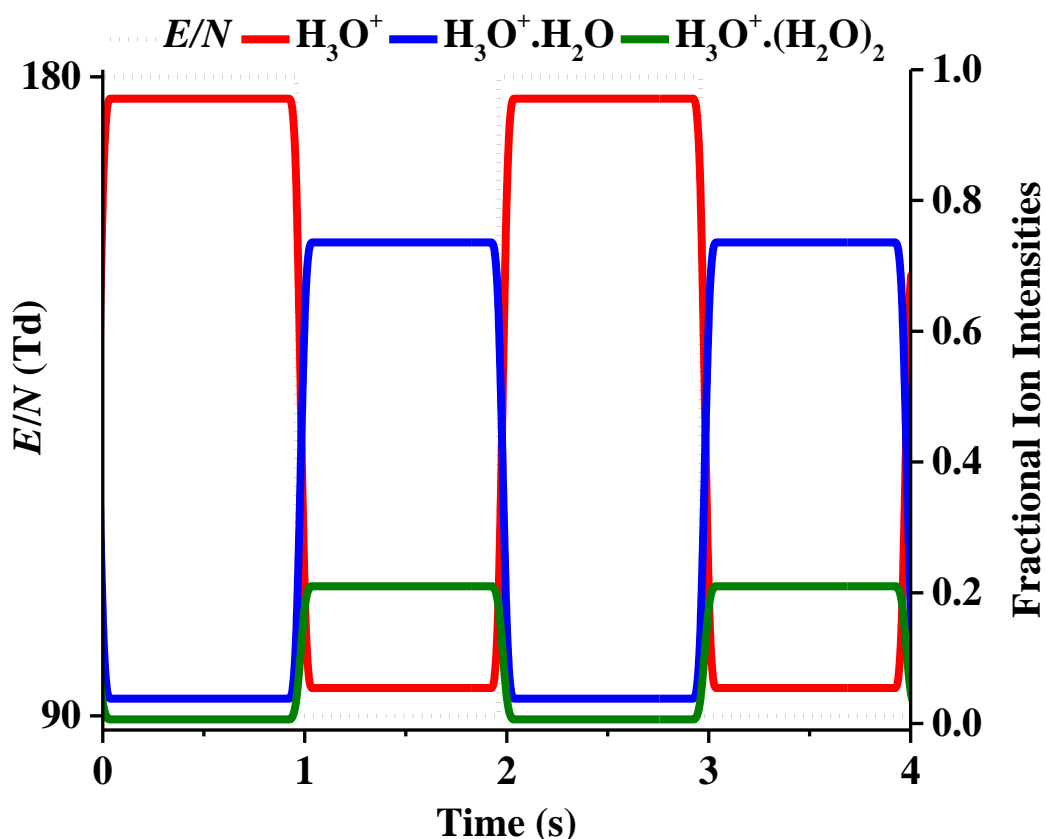
231 Figure 1 shows measurements of the fractional reagent ion signals (total ion signal adds  
232 up to 1) for  $\text{H}_3\text{O}^+$ ,  $\text{H}_3\text{O}^+\cdot\text{H}_2\text{O}$  and  $\text{H}_3\text{O}^+\cdot(\text{H}_2\text{O})_2$  for 180 Td and 90 Td switching at a frequency  
233 of approximately 1 Hz, starting with 180 Td at  $t = 0\text{s}$ . Figure 1(a) shows the raw data obtained  
234 from the instrument to illustrate the noise associated with 40 ms data acquisition and (b) the  
235 processed averaged data over the part of the cycle for which the ion signals have reached  
236 stability. The measured transition time when switching from a low to a high  $E$  value to result  
237 in 95% of the maximum ion signal was measured to be 60 ms. For changing from high to low  
238  $E$  values the transition time was measured as 140 ms to reach within 5% of the stable lowest  
239 ion signal for that  $E/N$  phase. In practice this limits the switching frequency to less than 5 Hz.  
240 However, we will demonstrate that that is more than adequate for applications to explosive  
241 detection, and hence to applications where the concentration of an analyte is changing over the  
242 time period of seconds.

243

244 (a)



245



247  
 248 **Figure 1.** Changes in the fractional ion intensities of protonated water and protonated water  
 249 clusters as  $E/N$  is switched between 180 Td and 80 Td at a frequency of 1 Hz showing (a) raw  
 250 data and (b) averaged ion intensities.

251

### 252 **Examples of Improved Selectivity: Explosive compounds**

253 **Product ion distributions as a function of the reduced electric field.** For any given  
 254 explosive, it is first necessary to ascertain the dependence of the product ion intensities as a  
 255 function of  $E/N$ , and hence determine which two  $E/N$  values should be used to enhance  
 256 selectivity. The dependences of the product ion distributions (PIDs) on  $E/N$  are required.  
 257 Therefore, in the following, not only are the characteristics of the switching reported, but also  
 258 details on the PIDs for 2,4-DNT, 2,6-DNT, HMTD, and RDX. However, it is important to  
 259 appreciate that the PIDs we have determined for different reduced electric fields are specific to  
 260 the KORE PTR-ToF-MS instrument and the operational conditions we have used. Owing to  
 261  $m/z$  dependence transmission of ions from a drift tube at a specific  $E/N$  to the transfer optics  
 262 and then through the mass spectrometer, differences in operational conditions (i.e. pressure and

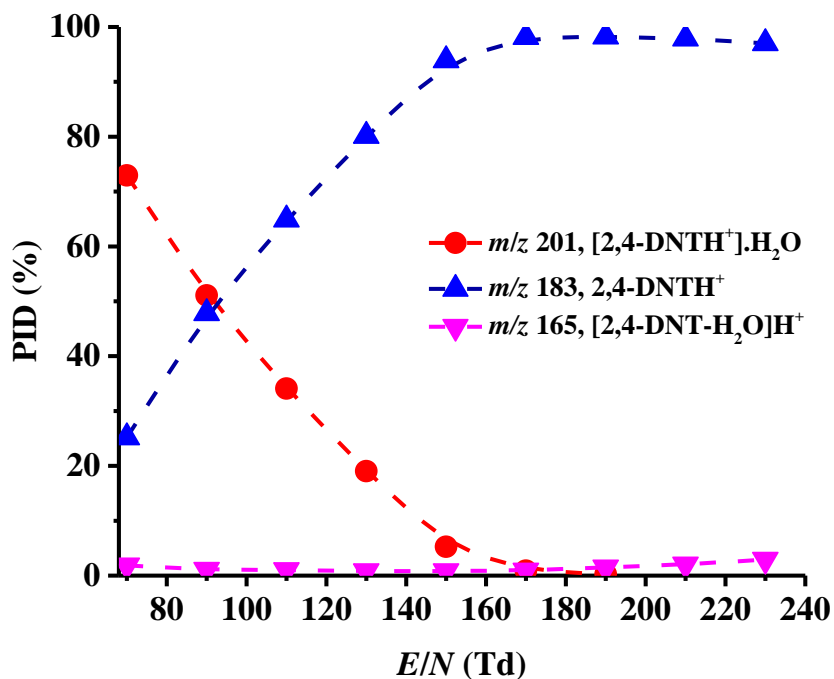
263 temperature), potential surface effects (e.g. stability of compounds e.g. reactions on metal  
264 surfaces or decomposition) and the rate of heating used for the thermal decomposition, different  
265 PIDs will result from the use of different conditions and instruments. Hence for a PTR-MS  
266 instrument to be of analytical use, the PIDs will need be determined for a given instrument  
267 under the set of conditions being used. The PIDs obtained and reported from PTR-MS studies  
268 should therefore include as much detail as possible, including information on any allowances  
269 used for transmission dependencies etc. For use in determining the probability of a given  
270 reaction pathway full details on  $m/z$  dependent transmission and detection sensitivity, thermal  
271 or reactive decomposition of the parent molecule, and effects of differences in operational  
272 conditions are required.

273 In the following the explosives' product ion distributions as a function of  $E/N$  have been  
274 obtained from the average of three background subtracted scans for each  $E/$ .

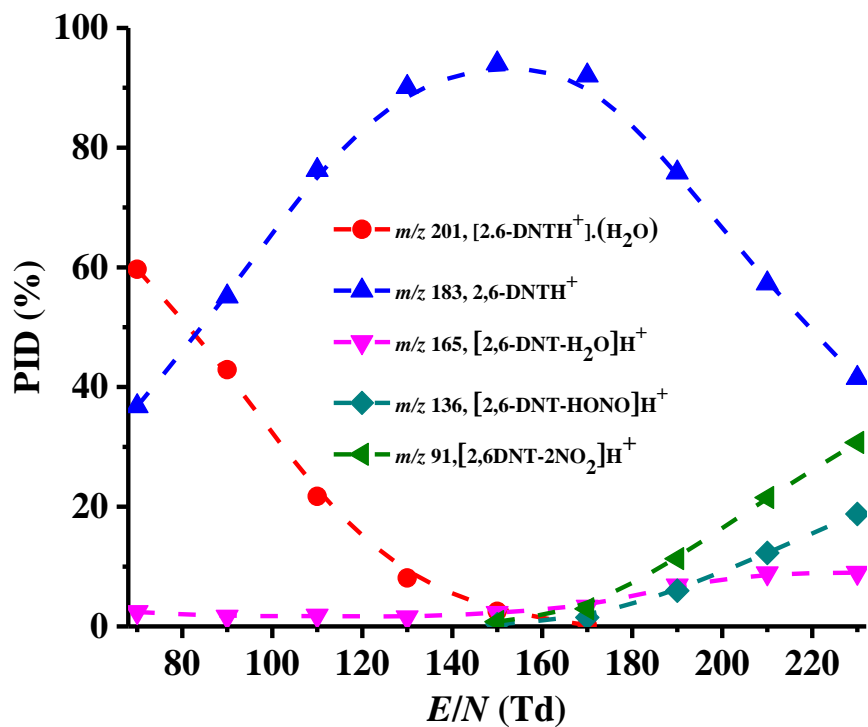
275 **2,4- and 2,6 dinitrotoluene ( $C_7H_6N_2O_4$ ).** Figure 2 shows the PID plot as a function of  $E/N$   
276 (70 - 230 Td) for (a) 2,4-DNT and (b) 2,6-DNT. (The product ion branching ratios for 2,6-DNT  
277 have already been published in another paper by us dealing with the applications of a radio  
278 frequency field in the drift tube.<sup>18</sup> However, for ease of comparison with the 2,4-DNT isomer  
279 the results are reproduced in this paper. The only difference is that the second water cluster  
280 ( $2,6\text{-DNT}^+(\text{H}_2\text{O})_2$ ) is not shown in figure 2(b), because its intensity is insignificant.)

281 From figures 2(a) and (b) it can be seen that monitoring product ions at  $m/z$  183.04 (the  
282 protonated parent) and 201.05 ( $\text{DNT}^+\text{H}_2\text{O}$ ) is sufficient for assigning 2,4-DNT, but that the  
283 presence of  $m/z$  136.04 (elimination of HONO from the protonated parent) and  $m/z$  91.06  
284 (elimination of two nitro groups) observed at the high  $E/N$  setting indicates the presence of 2,6-  
285 DNT. Another common ion detected for both isomers at high reduced electric field values is at  
286  $m/z$  165.05, which results from the elimination of  $\text{H}_2\text{O}$  from the protonated parent. Given that  
287 this is observed for both isomers, it cannot be used to differentiate the isomers.<sup>18</sup> A summary  
288 of results from the fast switching experiment for 2,4-DNT and 2,6-DNT are shown in figure 3,  
289 which show how the two isomers can be readily distinguished.

290  
291  
292  
293  
294  
295  
296

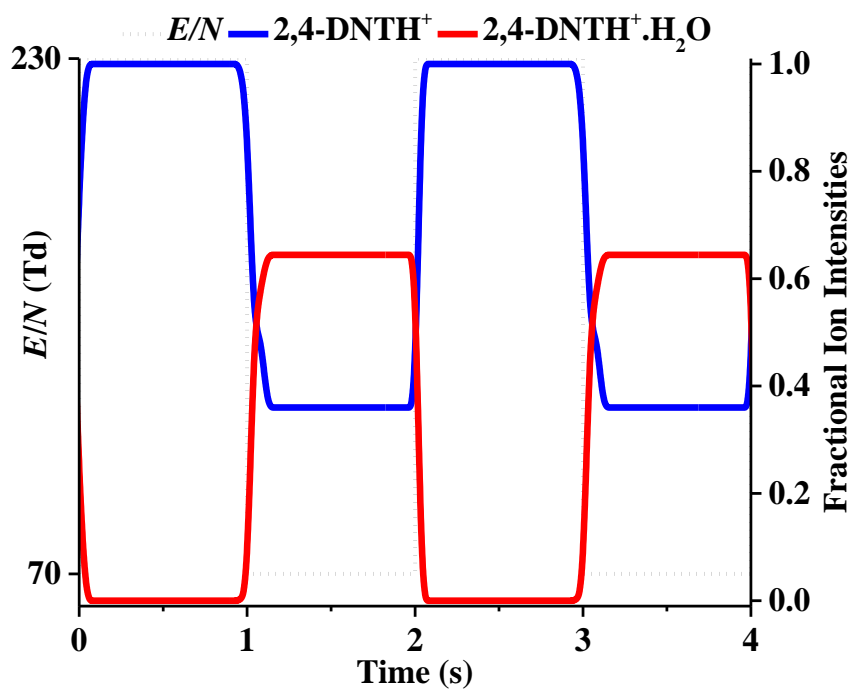


(b)

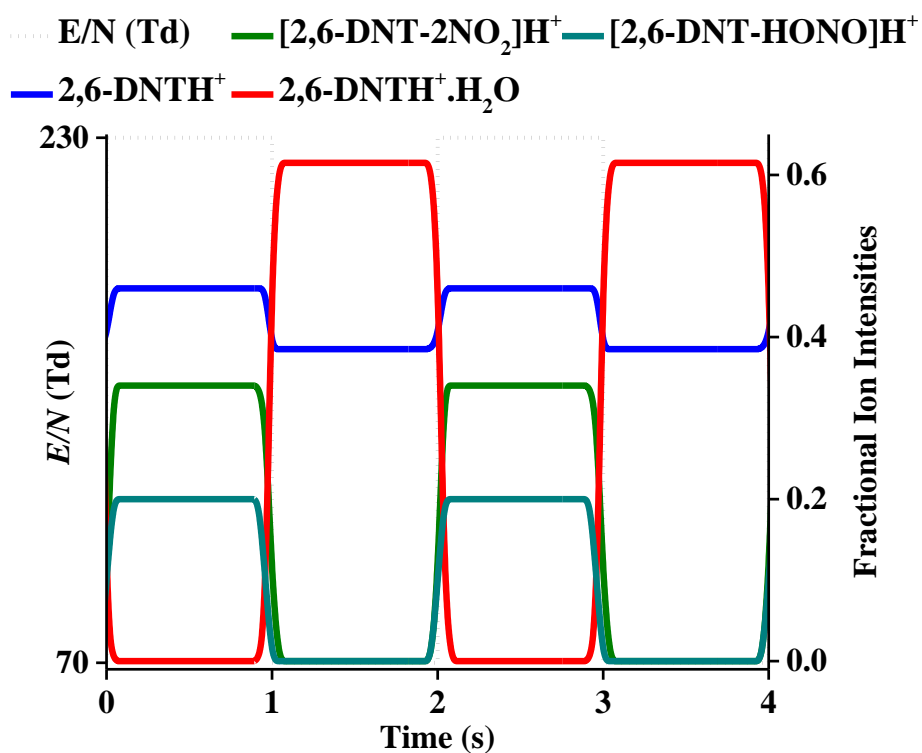


298 **Figure 2.** (a) Percentage product ion distribution (PID) results for (a) 2,4-DNT and (b) 2,6-  
 299 DNT as a function of reduced electric field (70 to 230 Td).

300 (a)



301 (b)



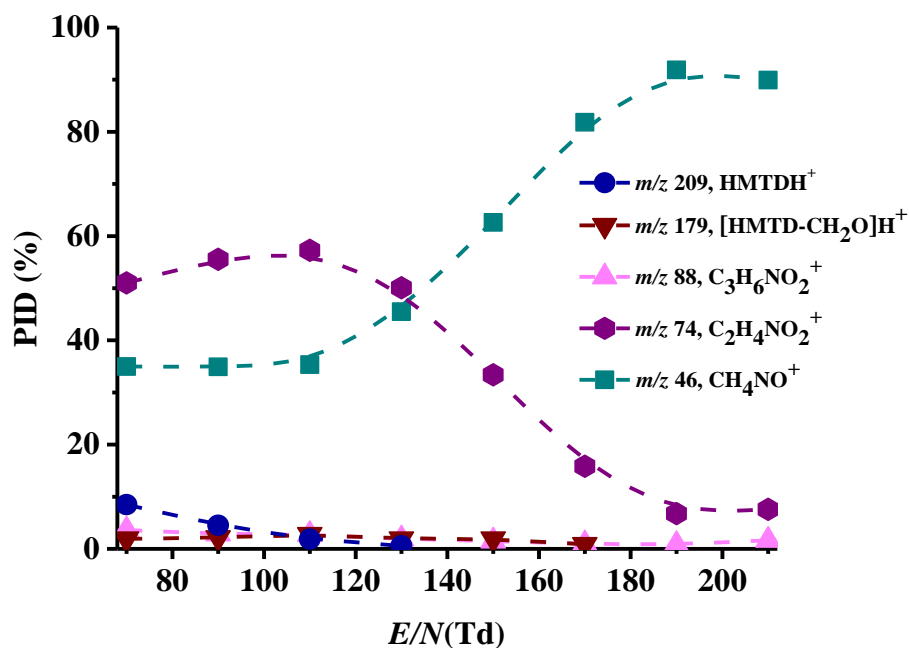
302

303 **Figure 3.** Changes in the fractional ion intensities averaged over each cycle using 1 Hz  $E/N$   
304 switching between 70 Td and 230 Td for (a) 2,4-DNT and (b) 2,6-DNT. The product ions at  
305  $m/z$  91.06 and  $m/z$  136.04 are distinctive of 2,6-DNT.

306 **HMTD (C<sub>6</sub>H<sub>12</sub>N<sub>2</sub>O<sub>6</sub>).** For HMTD five product ions are observed at  $m/z$  46.03, 74.02, 88.04,  
307 179.07 and 209.08. The product ions at  $m/z$  88.04 and  $m/z$  179.07 have negligible intensities at  
308 all  $E/N$  values, and are therefore not considered further.  $m/z$  209.08 is the protonated parent,  
309 but only has a reasonable intensity at low  $E/N$  ( $< 90$  Td). DFT calculations give  $877 \text{ kJ mol}^{-1}$   
310 and  $844 \text{ kJ mol}^{-1}$  as the proton affinity and gas-phase basicity, respectively, for HMTD. Thus  
311 proton transfer from not only protonated water but also from the protonated water clusters is  
312 exoergic. Given the high proton affinity of HMTD, the reaction of  $\text{H}_3\text{O}^+$  would most probably  
313 be dissociative, and the protonated parent is almost certainly a result of a reaction with  
314  $\text{H}_3\text{O}^+(\text{H}_2\text{O})_n$ . The product ion at  $m/z$  179.07 corresponds to the loss of formaldehyde ( $\text{CH}_2\text{O}$ )  
315 from the protonated parent, leaving  $\text{C}_5\text{H}_{10}\text{N}_2\text{O}_5\text{H}^+$ .  $m/z$  88.04 corresponds to  $\text{C}_3\text{H}_6\text{NO}_2^+$  and  
316  $m/z$  74.02 to  $\text{C}_2\text{H}_4\text{NO}_2^+$ . By taking advantage of the high mass resolution associated with  
317 KORE PTR-ToF-MS, we can rule out that the ion at  $m/z$  46.03 as being  $\text{NO}_2^+$ , because the peak  
318 position of that ion is at  $m/z$  45.99.  $\text{CH}_4\text{NO}^+$  agrees with  $m/z$  46.03. Given the significant  
319 rearrangement and eliminations required to produce this ion, and the fact that it has a high  
320 branching percentage even at low  $E/N$  (see figure 4(a)), it is possible that  $\text{CH}_4\text{NO}^+$  does not  
321 directly result from dissociative proton transfer to HMTD. It is probable that this ion is a  
322 consequence of the reaction of  $\text{H}_3\text{O}^+$  with a neutral product resulting from the thermal  
323 decomposition of HMTD in the system. Decomposition of HMTD could have resulted in the  
324 formation of other neutrals that then react with the reagent ions. However, initial temperature  
325 dependent measurements have not shown any dependence on the product ion distributions. The  
326 mechanism for the production of the product ions needs further exploration, but that is not the  
327 aim of this paper. Independent of the source of the product ions under the operation conditions  
328 we have used, and especially for  $m/z$  46.03, they are still specific to HMTD and hence we can  
329 use them to specify the presence of HMTD. Figure 4 (a) shows the PID obtained for HMTD as  
330 a function of the reduced electric field (70 - 210 Td). Under the experimental conditions used  
331 the product ions that dominate are at  $m/z$  46.03 and  $m/z$  74.02. However, the presence of the  
332 protonated parent observed at low  $E/N$  is a useful ion for identification although it is observed  
333 with a low branching percentage. Thus we have selected the product ions at  $m/z$  46.03, 74.02  
334 and 209.08 for use in identifying HMTD with a high specificity under our operational  
335 conditions. The switching results using these three product ions are shown in figure 4(b).

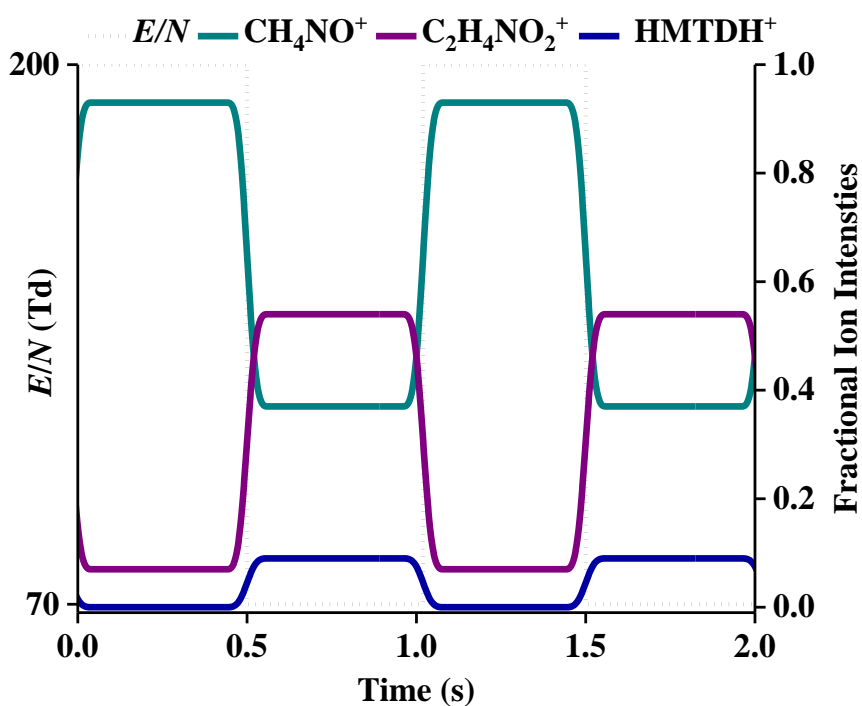
336  
337  
338  
339

340 (a)



341

342 (b)



343

344 **Figure 4.** (a) PID for HMTD as a function of reduced electric field covering the range 70-210

345 Td and (b) changes in the fractional ion intensities averaged over each cycle for a reduced

346 electric field switching 2 Hz. (2 Hz is presented here to illustrate the operation of the system as

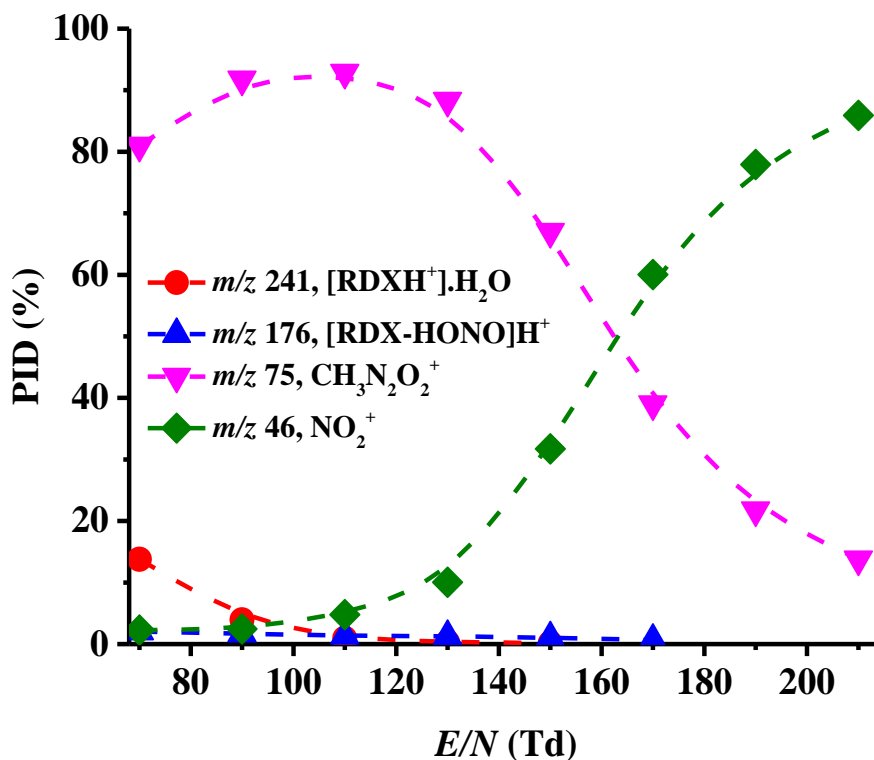
347 a different frequency.)



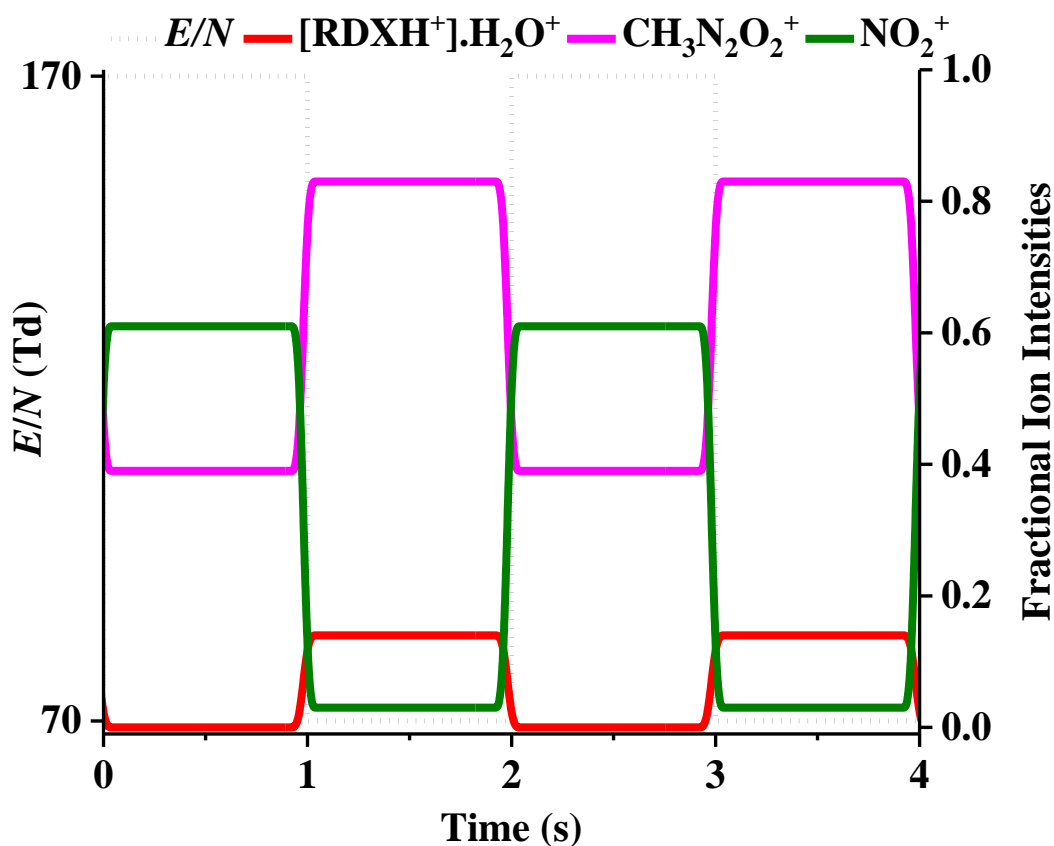
348 **RDX (C<sub>3</sub>H<sub>6</sub>N<sub>6</sub>O<sub>6</sub>)**. Major product ions are observed are at  $m/z$  45.99 (NO<sub>2</sub><sup>+</sup>) and  $m/z$  75.02  
 349 (CH<sub>3</sub>N<sub>2</sub>O<sub>2</sub><sup>+</sup>).  $m/z$  75.02 dominates for  $E/N < 160$  Td, whereas  $m/z$  45.99 dominates at for  $E/N$   
 350  $> 160$  Td. Another product ion is also observed at  $m/z$  176.04 ([RDX-HONO]H<sup>+</sup>) throughout  
 351 the  $E/N$  range investigated, but it only appears at a low intensity compared to the other two  
 352 primary product ions. At the lowest  $E/N$  an ion is observed at  $m/z$  241.05. This is assigned to  
 353 be RDXH<sup>+</sup>.H<sub>2</sub>O. Given the observation of this, it is surprising that no protonated monomer is  
 354 detected. We propose that as the reduced electric field is increased to the stage where no water  
 355 clustering occurs the protonated parent has too much internal energy for it to survive before  
 356 detection. DFT calculations give the PA and GB of RDX to be 764 kJ mol<sup>-1</sup> and 734 kJ mol<sup>-1</sup>,  
 357 respectively, and therefore only H<sub>3</sub>O<sup>+</sup> can efficiently react with RDX via proton transfer. Figure  
 358 5 (a) shows the PID for RDX as a function of  $E/N$  (70 – 210 Td) under the operational  
 359 conditions we have used. A separate study is being undertaken to investigate temperature  
 360 effects on the PID. For our operating temperatures, the PID shows that product ions at  $m/z$   
 361 45.99, 75.02 and 241.05 are sufficient to identify the presence of RDX with a high level of  
 362 confidence. Figure 5(b) shows the reduced electric field switching results for 70 Td and 170  
 363 Td.

364

365 (a)



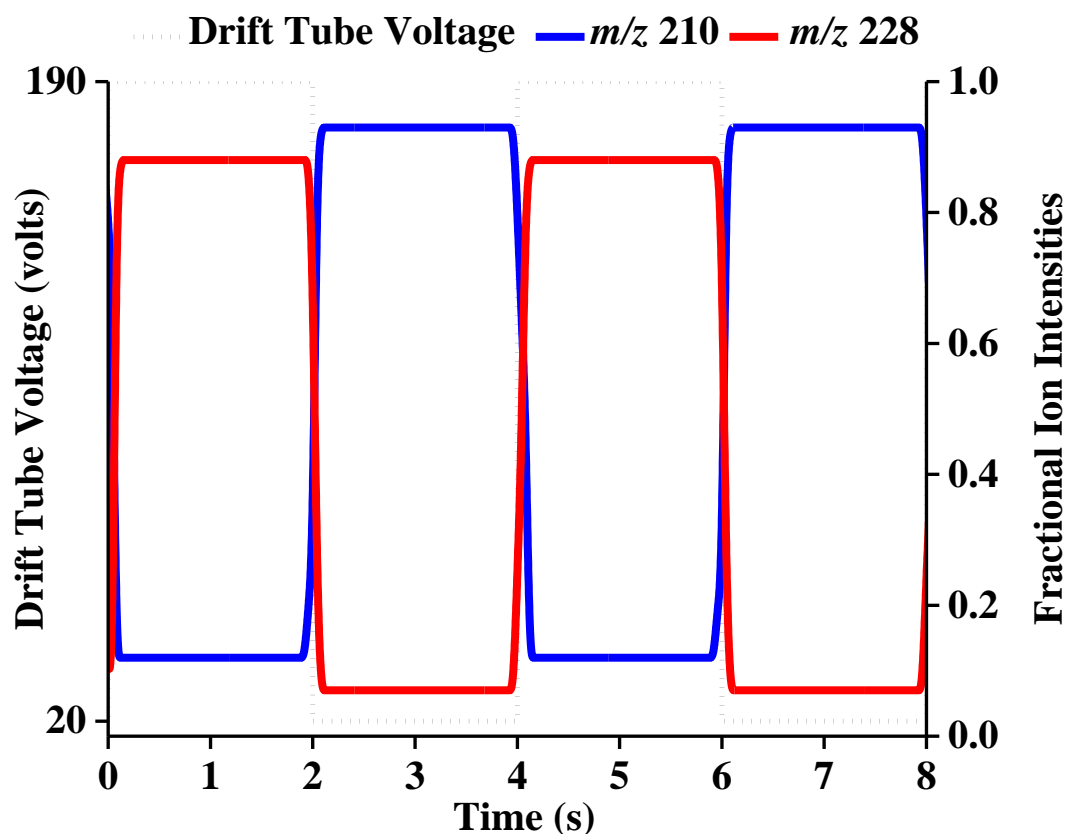
366



368  
 369 **Figure 5.** (a) PID for RDX as a function of reduced electric field covering the range 70-210  
 370 Td and (b) results for the reduced electric field switching at 1 Hz.

371  
 372 **Radio Frequency Ion Funnel and Drift Tube Voltage Switching: an Application to**  
 373 **TNT.** Recently, we demonstrated how a radio frequency ion funnel-drift tube (RFIF-DT) can  
 374 be employed in a novel way to modify the product ions resulting from the reaction of  $\text{H}_3\text{O}^+$   
 375 with TNT through changes in collisional induced dissociation.<sup>18</sup> In DC-only mode, and for all  
 376  $E/N$  values investigated, the reaction of  $\text{H}_3\text{O}^+$  with TNT leads to only one product ion, namely  
 377 protonated TNT at  $m/z$  228.03.<sup>8</sup> However, in RF-mode, another fragment ion is observed at  $m/z$   
 378 210.02, corresponding to the elimination of water from the protonated parent,<sup>18</sup> with the  
 379 intensity of this product ion increasing relative to the protonated parent with decreasing drift  
 380 tube voltage (i.e. decreasing  $E/N$  in DC mode). In that work we proposed that the dominance  
 381 of  $m/z$  210.02 at low drift tube voltages is a result of the protonated TNT spending a longer  
 382 time in the RF region of the drift tube. Through numerous collisional processes this allows it  
 383 to gain sufficient internal energy until it reaches a level that leads to the elimination of  $\text{H}_2\text{O}$ . In  
 384 this study we illustrate how improvements in selectivity can be achieved by combining RF-

385 mode with fast drift tube voltage switching for TNT (figure 6). We therefore propose that by  
386 combining the RFIF and drift tube voltage switching techniques an even higher confidence in  
387 the assignment of an analyte in a complex chemical environment may occur than is possible in  
388 DC-only mode.



389  
390 **Figure 6.** Application of combining radio frequency and fast drift tube voltage switching at 0.5  
391 Hz between 20 and 190 V (equivalent to 30 and 180 Td in DC-mode only) for reactions of  
392  $\text{H}_3\text{O}^+$  with TNT.

393  
394 **Conclusions**

395 We have successfully implemented new hardware and software to enable the rapid switching  
396 of the reduced electric field,  $E/N$ , with transition times less than 140 ms at frequencies of 0.1-  
397 5 Hz in the drift tube of a KORE Technology PTR-ToF-MS. This switching results in the rapid  
398 modification of product ions from the reactions of reagent ions with chemicals through changes  
399 in collisional energies. We have demonstrated in this paper how this technique provides an  
400 improved selectivity for a number of explosives, thereby leading to a higher confidence in  
401 identification.

402 The results show that for all explosive compounds investigated switching between for  
403 example 80 Td and 200 Td is sufficient for analytical purposes. Slightly different *E/N*s have  
404 been used in some of the examples provided in this paper, simply because they were found to  
405 provide the maximum signal, but in reality differences in intensities between 70 Td and 80 Td  
406 and 200 Td and 220 Td, for examples, are not significant.

407 By using TNT as an example, we have indicated how the combination of the new drift  
408 tube voltage switching capabilities with an RFIF DT provides further improvement in  
409 selectivity. This combination of switching capabilities and RFIF to PTR-MS opens up other  
410 possibilities for improved selectivity at little cost to the manufacture of the PTR-MS  
411 instrument.

412 The main conclusion that can be drawn from this work is that rapid reduced electric  
413 field switching adds a new dimension to the analytical capabilities of PTR-MS. And although  
414 demonstrated for explosive compounds in this paper, this innovation has of course applications  
415 outside of those for homeland security and can be used for any other sampling protocol where  
416 there are time restrictions in compound concentrations, e.g. where there are transient processes  
417 of where volatiles are present for a short period, such as occurs in real-time breath sampling,  
418 atmospheric pollution or emissions from leaf wounding.

419

## 420 **Acknowledgements**

421 We thank the Defence Science and Technology Laboratory for funding RGM under DSTL R-  
422 Cloud–Contract Number: DSTLX-1000096588 (Task Number: R1000100031). This research  
423 is part supported through a Marie Skłodowska-Curie Actions Innovative Training Network  
424 “IMPACT” supported by the European Commission’s HORIZON 2020 Programme under  
425 Grant Agreement Number 674911. The authors wish to thank Mahroz Mirzahekmati for  
426 producing the graphical abstract.

427

## 428 **References**

- 429 1. Ellis, A.M.; Mayhew, C. A. *Proton Transfer Reaction Mass Spectrometry: Principles and*  
430 *Applications*. 1<sup>st</sup> ed.; Wiley: 2014; Chichester, UK.
- 431 2. Cordell, R. L.; Willis, K. A.; Wyche, K. P.; Blake, R. S.; Ellis, A. M.; Monks, P. S. *Anal.*  
432 *Chem.* **2007**, *79*, 8359-8366.
- 433 3. Shen, C.; Li, J.; Han, H.; Wang, H.; Jiang, H.; Chu, Y. *Int. Journal of Mass Spectrom.* **2009**,  
434 *285*, 100-103.

435 4. Petersson, F.; Sulzer, P.; Mayhew, C. A.; Watts, P.; Jordan, A.; Märk, L.; Märk, T. D. *Rapid*  
436 *Comm. in Mass Spectrom.* **2009**, *23*, 3875-3880.

437 5. Mayhew, C. A.; Sulzer, P.; Petersson, F.; Haidacher, S.; Jordan, A.; Märk, L.; Watts, P.;  
438 Märk, T. D. *Int. Journal of Mass Spectrom* **2010**, *289*, 58-63.

439 6. Jürschik, S.; Sulzer, P.; Petersson, F.; Mayhew, C. A.; Jordan, A.; Agarwal, B.; Haidacher,  
440 S.; Seehauser, H.; Becker, K.; Märk, T. D. *Anal. Bioanal. Chem.* **2010**, *398*, 2813-2820.

441 7. Agarwal, B.; Petersson, F.; Jürschik, S.; Sulzer, P.; Jordan, A.; Märk, T. D.; Watts, P.;  
442 Mayhew, C. A. *Anal. Bioanal. Chem.* **2011**, *400*, 2631-2639.

443 8. Sulzer, P.; Petersson, F.; Agarwal, B.; Becker, K. H.; Jürschik, S.; Märk, T. D.; Perry, D.;  
444 Watts, P.; Mayhew, C. A. *Anal. Chem.* **2012**, *84*, 4161-4166.

445 9. Jürschik, S.; Agarwal, B.; Kassebacher, T.; Sulzer, P.; Mayhew, C. A.; Märk, T. D. *Journal*  
446 *of Mass Spectrom.* **2012**, *47*, 1092-1097.

447 10. Sulzer, P.; Jürschik, S.; Agarwal, B.; Kassebacher, T.; Hartungen, E.; Edtbauer, A.;  
448 Petersson, F.; Warmer, J.; Holl, G.; Perry, D.; Mayhew, C.; Märk, T. In *Future Security*,  
449 Aschenbruck, N.; Martini, P.; Meier, M.; Tölle, J., Eds. Springer Berlin Heidelberg: 2012; Vol.  
450 318, pp 366-375.

451 11. Kassebacher, T.; Sulzer, P.; Jürschik, S.; Hartungen, E.; Jordan, A.; Edtbauer, A.; Feil, S.;  
452 Hanel, G.; Jaksch, S.; Märk, L.; Mayhew, C. A.; Märk, T. D. *Rapid Comm. in Mass Spectrom.*  
453 **2013**, *27*, 325-332.

454 12. Lanza, M.; Acton, W. J.; Jürschik, S.; Sulzer, P.; Breiev, K.; Jordan, A.; Hartungen, E.;  
455 Hanel, G.; Märk, L.; Mayhew, C. A.; Märk, T. D. *Journal of Mass Spectrom.* **2013**, *48*, 1015-  
456 1018.

457 13. Sulzer, P.; Agarwal, B.; Jürschik, S.; Lanza, M.; Jordan, A.; Hartungen, E.; Hanel, G.;  
458 Märk, L.; Märk, T. D.; González-Méndez, R.; Watts, P.; Mayhew, C. A. *Int. Journal of Mass*  
459 *Spectrom.* **2013**, *354-355*, 123-128.

460 14. Acton, W. J.; Lanza, M.; Agarwal, B.; Jürschik, S.; Sulzer, P.; Breiev, K.; Jordan, A.;  
461 Hartungen, E.; Hanel, G.; Märk, L.; Mayhew, C. A.; Märk, T. D. *Int. Journal of Mass Spectrom.*  
462 **2014**, *360*, 28-38.

463 15. Agarwal, B.; González-Méndez, R.; Lanza, M.; Sulzer, P.; Märk, T. D.; Thomas, N.;  
464 Mayhew, C. A. *Journal of Phys. Chem. A* **2014**, *118*, 8229-8236.

465 16. Lanza, M.; Acton, W. J.; Sulzer, P.; Breiev, K.; Jürschik, S.; Jordan, A.; Hartungen, E.;  
466 Hanel, G.; Märk, L.; Märk, T. D.; Mayhew, C. A. *Journal of Mass Spectrom.* **2015**, *50*, 427-  
467 431.

468 17. González-Méndez, R.; Reich, D. F.; Mullock, S. J.; Corlett, C. A.; Mayhew, C. A. *Int.*  
469 *Journal of Mass Spectrom.* **2015**, 385, 13-18.

470 18. González-Méndez, R.; Watts, P.; Olivenza-León, D.; Reich, D. F.; Mullock, S. J.; Corlett,  
471 C. A.; Cairns, S.; Hickey, P.; Brookes, M.; Mayhew, C. A. *Anal. Chem.* **2016**, 88, 10624-10630.

472 19. González-Méndez, R.; Development and applications of Proton Transfer Reaction-Mass  
473 Spectrometry for Homeland Security: trace detection of explosives. PhD, University of  
474 Birmingham (2017).

475 20. Sulzer, P., Jordan, A., Märk, L., Mayhew, C. A., Becker, K., & Märk, T. D. *American*  
476 *Laboratory* **2011**, 43, 13-15.

477 21. Amador-Muñoz, O.; Misztal, P. K.; Weber, R.; Worton, D. R.; Zhang, H.; Drozd, G.;  
478 Goldstein, A. H. *Atmospheric Measurement Techniques* **2016**, 9, 5315

479 22. Hansel, A.; Jordan, A.; Holzinger, R.; Prazeller, P.; Vogel, W.; Lindinger, W. *Int. Journal*  
480 *of Mass Spectrom. and Ion Processes* **1995**, 149–150, 609-619.

481 23. Lindinger, W.; Hansel, A.; Jordan, A. *Int. Journal of Mass Spectrom. and Ion Processes*  
482 **1998**, 173, 191-241.

483 24. Fortner, E. C.; Knighton, W. B. *Rapid Communications in Mass Spectrometry* **2008**, 22,  
484 2597-2601.

485 25. Shen, C.; Li, J.; Wang, Y.; Wang, H.; Han, H.; Chu, Y. *International Journal of*  
486 *Environmental Analytical Chemistry* **2011**, 92, 289-301.

487 26. Misztal, P. K.; Heal, M. R.; Nemitz, E.; Cape, J. N. *Int. Journal of Mass Spectrom.* **2012**,  
488 310, 10-19.

489 27. Ennis, C. J.; Reynolds, J. C.; Keely, B. J.; Carpenter, L. J. *Int. Journal of Mass Spectrom.*  
490 **2005**, 247, 72-80.

491 28. Blake, R. S.; Whyte, C.; Hughes, C. O.; Ellis, A. M.; Monks, P. S. *Anal. Chem.* **2004**, 76,  
492 3841-3845.

493 29. Barber, S.; Blake, R. S.; White, I. R.; Monks, P. S.; Reich, F.; Mullock, S.; Ellis, A. M.,  
494 *Anal. Chem.* **2012**, 84, 5387-5391.

495 30. Frisch, M., Trucks, G., Schlegel, H., Scuseria, G., Robb, M., Cheeseman, J., Scalmani, G.,  
496 Barone, V., Mennucci, B., Petersson, G.: Gaussian 09, rev. A. 1. Gaussian Inc., Wallingford  
497 (2009).

498